Indian Journal of Engineering & Materials Sciences
Vol. 29, October 2022, pp. 598-604
DOI: 10.56042/ijems.v29i5.67616

Mechanical and Microstructural Evolution of Friction Stir Welded Joint of AA2014 Alloys

Bharat Singh[a*], Arvind Sankhla[b], Kuldeep K Saxena[a], & Piyush Singhal[a],

[a]Department of Mechanical Engineering, GLA University, Mathura UP India 281406

[b]Department of Mechanical Engineering, Nirma University, Ahmedabad Gujarat India 382481

Received: 25 January 2022; Accepted: 15 September 2022

The solidification cracking phenomenon restricts the use of fusion welding process to join aluminum and its alloy. Friction stir welding (FSW) process can be used in joining of aluminium alloys which is not or less susceptible to form welded voids, induced distortions, solidification cracking. In the present work an investigation of mechanical and microstructural changes after FSW is presented during the similar joining of AA2014 aluminium alloys. The influences of tool geometry during FSW is analysed and compared among the joint made by triangular, pedal and pentagonal pin. Based on the obtained mechanical properties of the joint metallurgical investigation is performed. Optical micrographs are used to reveal the phases present in the fusion zone. EBSD investigation of the selected sample is done to analyse the mis-orientaion angle and grain size etc. Pedal pin profile tool exhibit better mechanical properties in comparison to pentagonal pin and triangular pin. Obtained ultimate tensile strength and percentage elongation are 345MPa and 13.5 % respectively. Micro-hardness and impact energy are obtained as 125HV0.2 and 4.6 J of F_{pedal}sample. Obtained joint efficiency of Fpedal sample is 74%, which is higher among joint efficiency of Fpentagonal and Ftringular samples.

Keywords: FSW, AA2014, Recrystallization, Tensile properties, Pin profile, Grain refinement, Impact Energy, EBSD

1 Introduction

Aluminium shows high resistance to corrosion and better tensile properties[1,2]. A thick passivating film of aluminium oxide is formed instantly when it is exposed to atmosphere. Aluminium alloys are the non-flammable, thereby, can be utilised for applications involving flammable or explosive material handling[3]. High machinability and workability are one of the important characteristics of aluminium and its alloys. It is commonly used for a large variety of industrial applications due to wide benefits in terms of strength, light weight of aluminium alloys[4]. Aluminium alloyAA2014 is used widely in aerospace, automotive applications, and light weight structural applications. Increasing demand of the structural applications of AA2014, increases the fabrication requirement[5]. Presence of high reactivity, thermal conductivity, and coefficient of thermal-expansion make these alloys difficult to fabricate by the application of heat. In fusion welding process the heat input has the key role to decide the joint property[2,6]. Heat associated in the conventional welding lead to high residual stress and thereby high distortion[7]. These issues can be avoided or minimised by using friction assisted welding where the heat associated with the process is comparatively less[8,9]. Friction stir welding process was invented and utilised by TWI in 1991[10]. The technique emerged as one of finest process for aluminium joining process, which make use of a probe tool consisting three segments named as probe, shoulder and shank of the tool[11,12]. Frictional heat is generated between the faying surfaces because of direct contact of pin and shoulder which decides the flow of material. Plasticised material flow is key indicator for the obtained mechanical properties[13]. The quality of joint made is greatly influenced by the plasticised material flow which is majorly depends upon the tool pin profile.It is observed from the literature that welding zone possess approximately 420-500°C temperature[14]. Many researches are reported the influence of pin profiles during FSW of aluminium alloys and observed significant change in the strength of the joint[15-17,11]. Other process parameters such as transverse speed, rotational speed and tilt angle etcalso plays an important role in deciding the microstructure[2]. Padmanaban et al.[18] studied the influences the FSW process parameters dissimilar joining of AA2024 and AA7075 and revealed that defect free joints are formed

*Corresponding author (E-mail: singhbharat09@gmail.com)

with rotational speed of 1050 rpm.Veljic et al.[19] investigated the thermos-mechanical behaviour of FSW process and observed that high rotational speed reduces the intensity of friction heating of the specimen while the heat generated by plastic deformation increases. It is observed that for aluminium alloys, FSW is most suitable process for joining in comparison to fusion welding. Tensile strength obtained using FSW better than strength obtained in fusion welding[20].

In the present work, an experimental study is performed to analyse the obtained mechanical and microstructural properties of the joint made by different pins. The influences of pin profiles are presented and discussed. Further, optical and EBSD analysis of the best tool, obtained based on the mechanical properties, is conducted.

2 Materials and Methods

In the present study two similar plates of AA2014 aluminium alloys are joined using friction stir welding. The chemical composition of the base material AA2014 (weight %) is Cu -4.1, Fe-0.2, Si-0.6, Mg-0.5, Cr-0.01, Zn-0.14, Ti-0.05, Al- remainder. Specimen is cut from 5mm sheet of dimensions 200 x50 mm. Faying surface of specimens are chemically cleaned using acetone. Thermo-physical and mechanical properties of the as received material are as follows, density-2.78 gm/cm^3, Young's modulus-73 GPa, UTS-462, yield strength -351MPa, elongation at break- 18.5%, Micro hardness (Vickers)-135HV.

In order to perform welding, tools are prepared from H13 die steel as per the pre decided dimensions. Die steel H13 possess excellent combination of high toughness, high harden ability and resistance to thermal cracking. Prepared samples are undergone heat treatment process followed by quenching (oil) to further improve the wear resistance and hardness. FSW tool parameters are used as tool probe length-4.2mm, shoulder diameter-24mm, shoulder concavity-20. Three different probe profiles are used as triangular, pedal and pentagonal as given in Fig. 1(a-c).

Friction stir welding is performed using a modified vertical machine with optimized process parameters of FSW. Other selected process parameters for welding are rotational speed-1025 rpm, welding traverse speed-100mm/min, plunge force -3.5kN, Tilt angle- 20 and backing plate material-mild steel. These process parameters are taken uniform in all welding. In order to arrest all degree of freedom, plates are held together firmly by using a fixture (mechanically operated) to withstand the generated plunging force. Friction stirred samples are categorized based on the tool used. Sample welded by triangular, pedal and pentagonal pin are coded as $F_{triangular}$, F_{pedal}, $F_{pentagonal}$ as presented in Fig. 1(a & c) respectively.

Micro hardness of the joints, those prepared by different pin profiles are measured using Truemet Micro Vickers hardness tester. The specimen is cut transversely from the welded joint. A sample for micro hardness testing are prepared using metallographic practice (polished by emery paper to 4/0 and followed by cloth polishing) is used to prepare the sample for micro hardness test. Micro hardness testing is performed on the midsection of the prepared samples with a test load 200 gm. Charpy Impact testing is performed to evaluate the impact energy of the welded samples. The samples are prepared as per the ASTM E23 standard as per the dimensions 55 x 10 of 5 mm. Transversely sectioned specimen is provided with a notch of 2 mm width and 0.25 root radius with 45^0 groove angles. Tensile properties of the as welded specimens are measured using Tensile testing machine at room temperature. Test coupons are prepared as per the ASTM E8 guidelines from the transversely cut welded joint. The obtained load- extension data is used for calculating the ultimate tensile strength (UTS), percentage elongation and joint efficiency etc. Optical microscopy and electron beam scatter diffraction

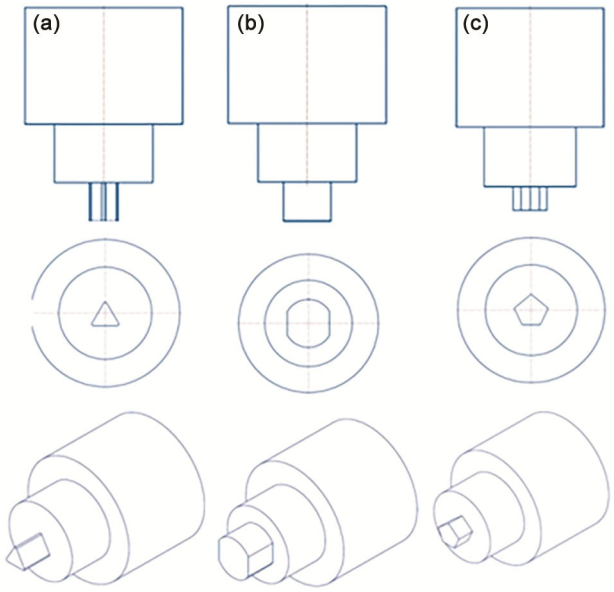

Fig. 1 — Friction stir welding pin profiles to perform the friction stir welding on similar AA 2014 aluminum alloys sample a) triangular pin, b) pedal pin, and c) pentagonal pin.

(EBSD) measurement are performed to analysis metallurgical changes after welding. Samples are prepared as per the standard procedure. For etching of the samples, solution of Keller's reagents is used. For EBSD analysis, after mechanical polishing, samples were electro-polished using Buehler ElectroMet® 4 Polisher-Etcher. For EBSD measurements, a scanning electron microscope FEI model Quanta™ 3D FEG was used. Obtained data after scanning further analyzed using TSL OIM software. In order to specified the microstructural entity, 2000 grains were taken. Grain size, angle of misorientations, grain orientation spread(GOS), grain boundaries distributionis then measured and presented. Harmonic series expansion method is used to plot the Inverse pole figure (IPF) and are presented normal to compression axis. Low angle grain boundary (LAGB) and high angle grain boundaries (HAGB) are specified with a misorientation angle between 1 to 15° as LAGB and misorientation>15° as HAGB.

3 Result and Discussion

In FSW process, tool pin profile plays a vital role in deciding the microstructural properties and hence the obtained mechanical properties. Profiles of tool pin affects the geneartion of heat and dynamic material flow in the plasticised form. The geometry of the tool has a direct influence on the degree of intermixing of faying surfaces and the extent of the weld region. The properties obatined based on different pin profiles are measured, presneted and discussed in the section.

3.1 Tensile Properties

Transverse tensile properties of welded samples are measured in terms UTS, % elongation and calculated joint efficiency. The joint efficiency is calculated based on the FSW joint strength to the strength of the parent metal.All above properties are extracted from the obatined true stress – strain graph presnted in Fig. 2, which shows tensile testing results based on the different tool pin profile .

Tabulated properties are avergae of the three measured values to ensure the accuracy. Observed deviation of individual strength from the avergae value of strength is ±5 MPa. Whereas in variation found in percentage elongation is ±0.5 from the average value.

As recived parent metal is exhbiting the UTS value 466 ±5 MPa and percentage elongation 18.5 ± 0.5%. The tensile strength obatined using triangular pin is 315 MPa, which is 32% less than the unwelded base material whereas percentage elongation is 54% lower than the as received parent metal (PM). The calculated joint efficiency of the welded sample using triangular pin is 67% as presented in Table 1

Lower tensile strength of the welded samples using triangular pin showed the poor joint efficiency. The specimen welded with pedal pin exhibits tensile strength as 345 MPa which is 26% lower than the as received PM as shown in Fig. 3a

Ductility in terms of percentage elongation measured of the welded sample using pedal is lowered by 27% in comparison to PM as shown in Fig. 3b. Better tensile strength and percentage elongation are noticed using tool with pedal pin profile in comparison to other tool pin profiles. Percentage elongation of welded sample using pedal pin is 13.5% as presented in Table 2.

It can be seen from the result that welded joint using pedal pin profile showed higher value of percentage elongation and tensile strength in comparison to other pin such as triangular and

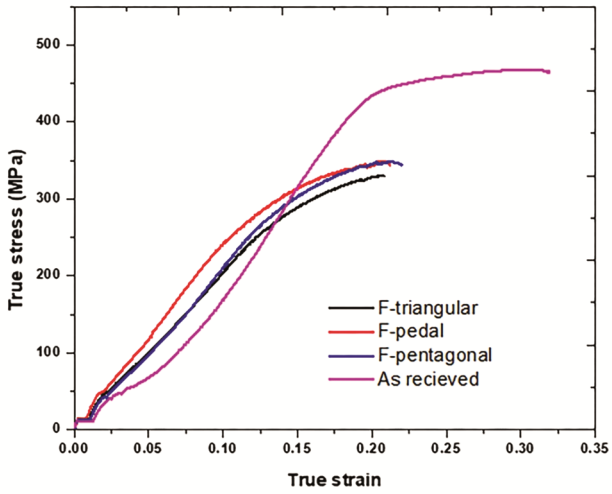

Fig. 2 — Tensile true stress- true strain graph of transverse samples of welded joint.

Table 1 — Recorded tensile properties of the the joints such as ultimate tensile strength and joint efficiency

Type Pin Profile	Coded name	UTS (MPa) ±10MPa	Joint Efficiency %
Triangular Probe	$F_{triangular}$	315	67
Pedal Probe	F_{pedal}	345	74
Pentagonal Probe	$F_{pentagonal}$	332	71
Base metal	As received	466	-

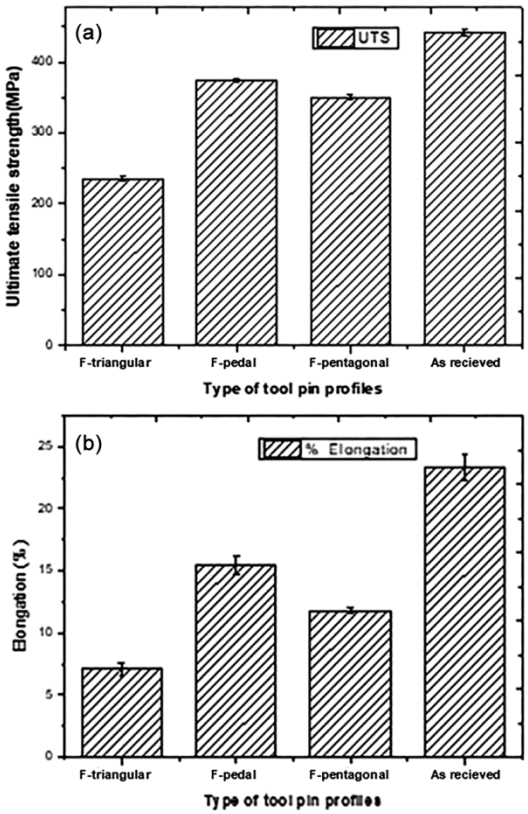

Fig. 3 — Obtained tensile properties after tensile test a)UTS; b) % elongation.

Table 2 — Measured percentage elongation of FSWed of AA2014

Type Pin Profile	Coded name	% Elongation) ±0.5%
Triangular Probe	$F_{triangular}$	8.4
Pedal Probe	F_{pedal}	13.5
Pentagonal Probe	$F_{pentagonal}$	11.2
Base metal	As received	18.5

pentagonal pin profiles. It is well noticed that tensile properties of the welded joint showed lower value than the as received parent material. It can be attributed due to over aged microstructure and deformation locally in heat affected zone. Coarsening of formed precipitates in heat affected zone could the reason of lower tensile strength and ductility. Tensile fracture is observed in the retreating side of in all welded samples. It can be attributed due to formation of wide low hardness zone in the retreating side. Pedal tool pin profile has flats without sharp corners. Flats with no sharp edge on the tools has better pulsating action which accompanied with improved plastic deformation and material flow. Generation of heat due to frictional heating is majorly influenced by severe plastic deformation and resultant material flow. So obtained mechanical properties using pedal pin is

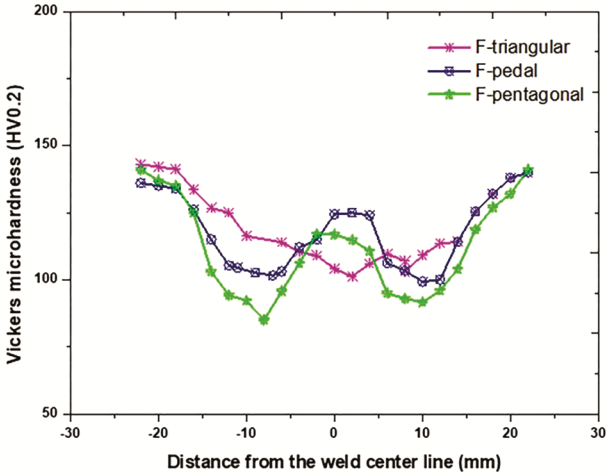

Fig. 4 — Variation in micro hardness of the welded samples.

the result of better pulsating action, smooth flow of material and generation of heat.

3.2 Micro hardness Variation

Vickers micro hardness are recorded at the mid thickness of cross section (transverse) of FSW joints. Samples are prepared as per ASTM E384 guidelines of friction stir welded joint. It is well clear that hardness graphs are showing 'W' shape distribution in all welded samples as presented in Fig. 4. Plotted micro hardness values are the average of three reading to ensure the accuracy. The pattern clearly indicates the variation in hardness distribution along the heat affected zone (HAZ), thermomechanical affected zone (TMAZ) and stirred zone(SZ). Measured value of micro hardness of parent metal is 135±5 HV0.2. Hardness values of all welded samples i.e. $F_{triangular}$, F_{pedal}, $F_{pentagonal}$, are significantly decreased in comparison to parent metal. It is found in the friction stir welded samples that strain hardening strengthening of the material is reduced notably because of dynamic recrystallization. Intensity heat distribution during welding in different region of joints also play a vital role in deciding the low hardness zone. However, type of pin profiles and other parameters of FSW determine the heat distribution in stirred zone.

It is observed from the Fig 4. that micro hardness of the welded samples in SZ by using triangular pin ($F_{triangular}$) is 107 HV0.2, which shows 20% reduction in the micro hardness in comparison to base metal. The hardness of the sample obtained using pedal pin(F_{pedal}) exhibiting 125 HV0.2, which is 14.4% higher than the $F_{triangular}$. However, F_{pedal} sample shows the hardness values lower than the parent metal.

Since, sample welded with pentagonal pin showed moderate hardness values in comparison to triangular and pedal pin. $F_{pentagonal}$ possess 118HV0.2 micro hardness in the stir zone which is 13% lower than the hardness of parent metal. The hardness distribution in the TMAZ and HAZ is lower than the parent hardness. It can be attributed that reduction in hardness values in SZ is the result of heat distribution which ultimately dissolve the precipitates during the dynamic recrystallization. The heterogeneous distribution of grain size in the weld joint from top to bottom of the joint, results in loss of hardness in the stir zone and nearby regions[21].

3.3 Impact Energy variation of the FSWed samples

Impact strength represents the capability of the material to resist deformation till its failure. Charpy impact test was performed to determine the impact energy of welded joint made by using different pins. Test coupon are made as per the ASTM E23 standard for test.

It is observed from the results that impact energy of joints are significantly decreased after FSW. As received parent metal showed 8.9J impact energy before welding. $F_{triangular}$ sample is exhibiting 2.75J impact energy which is the lowest value of impact energy among other samples i.e. F_{pedal} and $F_{pentagonal}$as presented in Fig. 5.

Figure 5, clearly reveals that the welded joint made by pedal pin showing highest values impact energy. However, the value of impact energy obtained using the pedal pin is lower than the parent metal. Based on the above results and discussion it is clear that F_{pedal} samples exhibiting better mechanical properties in terms of hardness, tensile and impact strength. So, to understand in depth phenomenon behind the samples, metallurgical microscopy and EBSD analysis is performed and discussed of F_{pedal} samples.

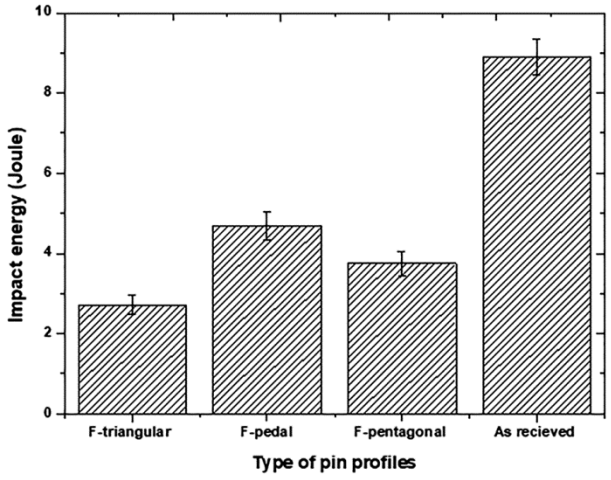

Fig. 5 — Variation of Impact energy with tool pin.

3.4 Optical Microscopy Analysis

FSWed joints made by pedal pin profiles are further studied and analysed. From FSWed samples it can be found that welded joint showed no discontinuities and better material flow on the top of SZ. Optical micrograph of the F_{pedal} sample is presented in Fig. 6. Figure 6(a), represent micrograph of parent metal in as received conditions. Whereas, micrograph of the welded sample is presented in the Fig. 6(b). Figure 6(b), shows the distribution of intermetallic compound formed when exposed to heating and cooling. The distribution of precipitates is non uniform across the stirred zone. These second phase particles are also responsible for strengthening. Observed region in welded zone has varied microstructure due to distribution heat in the region. It is observed that stirred zone exposed to maximum frictional heating due to direct contact of plasticised material to tool shoulder and pin profiles. In SZ, plasticised flow of material and subsequent heating of zone resulted in microstructural changes which ultimate alter the grains size in the region. The zone close to SZ is termed as TMAZ, where the distribution of heat to this region alter the microstructure and grain size in both side i.e. advancing side and retreating side. From microstructural graphs, it is observed that SZ exhibits equi-axed grains where as TMAZ zone shows elongated grains in comparison to SZ. The pin profile has major contribution in heat distribution in different welding zones.

3.5 EBSD Analysis of F_{pedal} sample

In order to understand the in depth investigation of the welded joint, EBSD analysis is performed. Misorientation angle, grain boundaries, grain size and inverse pole figures are presented based on the EBSD

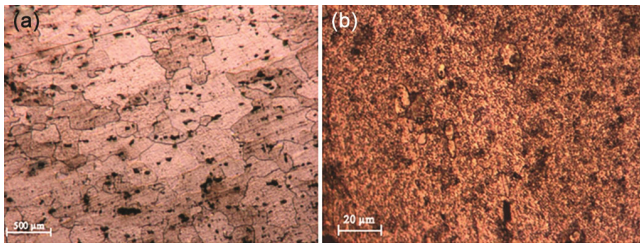

Fig. 6 — Micrograph of welded samples a) as received parent metal, and b) welded stirred zone.

analysis. Inverse pole figures, shows equi axed microstructure in stirred zone as presented in Fig. 7a. it is also observed from the EBSD analysis that less sub grains are found in the microstructure. In stirred zone, there is variation of grain size locally and the high angle grain boundaries appear more in the stirred zone. Figure 7(a), clearly reveals dynamic recrystallization in the obtained microstructure.

Figure 7(a), also represent the transition of the stirred zone and thermomechanical affected zone, which possess different microstructure at the interface. TMAZ in advancing side shows the large elongated grains with low angle grain boundaries partially as presented in Fig. 7(b). However, TMAZ advancing side high angle grain boundaries with partial sub grains are observed. The partial distribution of elongated grains in both sides of TMAZ, found because of the partial recrystallization of the structure. Partial recrystallization of microstructure is observed due to extent of heating of the TMAZ near to SZ. TMAZ of retreating side exhibits similar pattern of microstructure except the grain size distribution as presented in Fig. 7(c). Figure 7(c), depicts the retreating side of the TMAZ, which shows larger grains in comparison to TMAZ-advancing side.

The distribution of grain size with area fraction is presented in Fig. 8. Figure 8, shows the grain size in distribution stirred zone, advancing and retreating side of the TMAZ. In Stirred zone, maximum area of fraction possesses grain size in between 2.5 µm to 13.5 µm. It is evident that lower grain size result in better strength the material as per the Hall Petch theory as written in Eq. 1[22].

$$\sigma_y = \sigma_0 + \frac{k_y}{d^{\frac{1}{2}}} + \text{Density of dislocation (Eq.1)}$$

where σ_y = Yield strength in MPa, σ_0 = constant (Material) for starting stress, k_y = Strengthening coefficient, d = grain size (diameter)

Stirred zone shows average grain size 8.5 µm which also justify the results of hardness where in comparison to TMAZ, SZ shows better hardness values. From the grain size distribution curve, it is well clear that average grain size of both side of TMAZ is greater than the average grain size of the SZ.

In order to determine the role of grain size on the strengthening of the material, two important parameters such as grain size and density of dislocations are considered and given in Eq. 1. It is well clear that parent metal showing better strength in comparison to SZ, even after having lower size of grain (SZ). It is reported in the literature that during friction stir processing/welding, density of dislocations decreased significantly[23]. It reduces the effect of work hardening of the material. Reason for reduction in dislocation density is because of continuous dynamic recrystallization. It is observed that dynamic recrystallization is found easier in materials having high stacking fault energy (HSFE). Aluminum is especially AA2014 is consider as HSFE

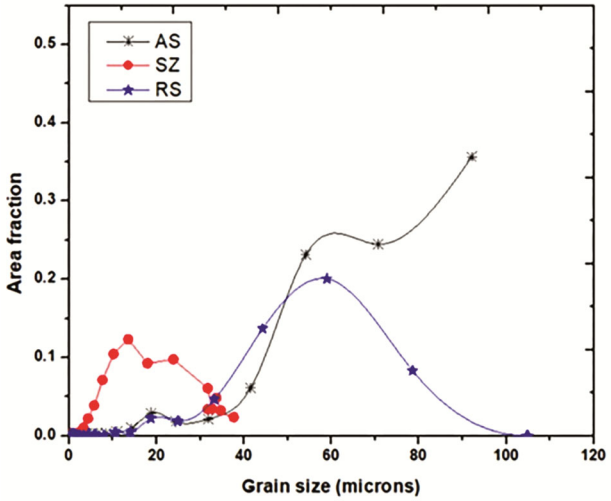

Fig. 8 — Obtained grain size of microstructure of F_{pedal} sample showing the grain size area fraction distribution along SZ , advancing side, retreating side.

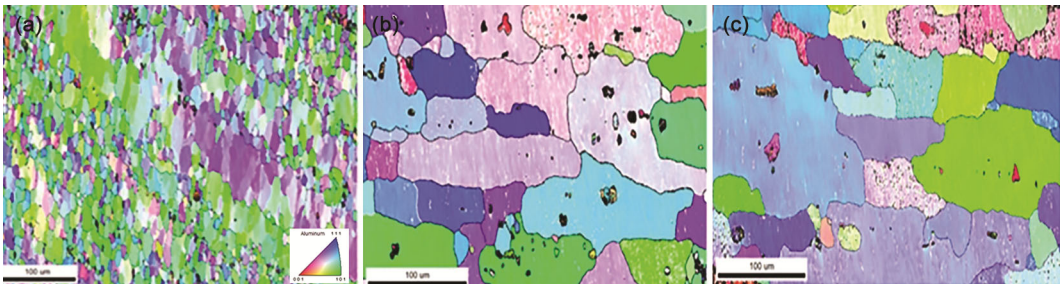

Fig. 7 — Inverse pole figure (IPF)of welded joint made by pedal pin profiles showing a) SZ, b) TMAZ-advancing side, and c) TMAZ-retreating side.

material, which increase the chances recrystallization at elevated temperatures. New grains are formed when the material is exposed to dynamic recrystallization by progressive and continuous increase in low angle grain boundaries. High angle grain boundaries are increased if this progressive recrystallization increased. Eventually, high angle grain boundaries are favorable for strengthening, which creates hindrance in dislocation movement. Hence, increase the work hardening properties.

4 Conclusions

The present study summarized the experimental work carried out to investigated mechanical and microstructural behavior of the AA2014 FSWed joint, also determine the defect tool pin for the joining of AA2014.

a) The obtained mechanical properties of the FSWed joint are less than the parent metal. It is because of decreased dislocation density in the microstructure.
b) Pedal pin profile tool exhibit better mechanical properties in comparison to pentagonal pin and triangular pin. Obtained ultimate tensile strength and percentage elongation are 345MPa and 13.5 % respectively. Micro-hardness and impact energy are obtained as 125HV0.2 and 4.6 J of F_{pedal} sample.
c) Obtained joint efficiency of F_{pedal} sample is 74%, higher than $F_{pentagonal}$ and $F_{tringular}$ samples.
d) Smooth pulsating effect of pedal pin profile shows better material flow and distribution of heat, which eliminate the chances of tunnel effect.
e) EBSD analysis shows that SZ possess lower grain size in comparison to both side of TMAZ. Equi-axed grain structure is obtained in stirred zone with average grain size 8.5 μm. The equi-axed structure is the result of continuous dynamic recrystallization observed in FSW.

References

1 Jacquin D & Guillemot G, *J Mater Proces Tech*, 288 (2021)116.
2 Singh B, Singhal P, & Saxena K K, *Adv Mater Proces Tech*, 6 (2020) 1.
3 Polmear I J, *Light Alloys: Metallurgy of the Light Metals*, (Arnold Publication London) 3rd Edn 1995, p.1
4 Scerra M, Global aluminum consumption from 2016 to 2023 *Report, Statista*, 2020.
5 Stojanovic B, Bukvic M, & Epler I, *App Eng Letters*, 3 (2018) 52.
6 Shuang-Jian Y, Chen D K, Jiang T L, Kun C W L & Li Y Z J, *Acta Meta Sinica*, 33(2020) 1032.
7 De A & Deb Roy T, *Sci Tech Welding Joining*, 16 (2011) 204.
8 Mori K & Abe Y, *Int J Lightweight Matand Manuf,* 1 (2018) 1.
9 Chaudhari A N, Dixit K, Bhatia G S, Singh B, Singhal P, & Saxena K K, *Mater Today Proc,* 28 (2019) 1314.
10 Thomas W M, Nicholas E D, Needham J C, Murch M G, Smith P T, & Dawes C J, *Int J Mater Forming,* 3 (2010) 1079.
11 Singh B, Saxena K K, Singhal P & Joshi T C, *J Mater Eng and Perf*, 30 (2021) 8606.
12 Su H, Xue L & Wu C, *Int J Adv Manuf Tech,* 108 (2020) 1.
13 Nandan R, Deb Roy T & Bhadeshia H K D H, *Prog Mater Sci,* 53(2008) 980.
14 Eramah A M & Rakin M P, *Thermal Sci* 18 (2014) 21.
15 Sahu P K & Pal S, *Mat Manuf Proc* 33(2018) 288.
16 Sharma A N, Siddiquee Z A K, & Mohammed M T, *Mat Manuf Proc* 33 (2018) 786.
17 Tamadon A,Baghestani A, & Bajgholi M E, *Tech* 8 (2020) 1.
18 R Padmanaban R, V. Balusamy V & Vignesh R V, *Materwiss. Werksttech* 51 (2020) p.17.
19 Marko D M, Sedmak R A & Radovic N, *Thermal Sci 00* (2021)186.
20 Singh B, Sharma S, Kumar V, Maheshwari K & Singhal P, *IOP Conf Series: Mater Sci and Eng,* 1116 (2021) 012080.
21 Dixit V, Mishra R S, Lederich R J & Talwar R, *Sci Techn Welding Joining*14(2009) 346.
22 Naik S N & Walley S M, *J of Mater Sci* 55(2020) 2661.
23 Malakar A, Suresh K S, Pancholi V, Brokmeier H G & Schell N, *Mater Characterization* 167 (2020) 1.